Supplementary Material: In-situ ESEM imaging of the vapour pressure dependent sublimation-induced morphology of ice

Malavika Nair, Anke Husmann, Ruth E. Cameron,* and Serena M. Best†

Cambridge Centre for Medical Materials,

Department of Materials Science and Metallurgy,

University of Cambridge, 27 Charles Babbage Road,

Cambridge, CB3 0FS, United Kingdom

(Dated: March 16, 2018)

* rec11@cam.ac.uk

† smb51@cam.ac.uk

I. FROST VS. ICE

The distinction between frost and the ice considered in this work is an important one to make, predominantly due to the vast microstructural differences arising from the growth process. The solute driven growth of frost produces highly faceted and large single crystals with distinct dendritic growth (Figure 1) whereas the thermally driven growth of ice does not exhibit such faceting due to the more subdued length scale of thermal noise that drives dendritic growth in ice.

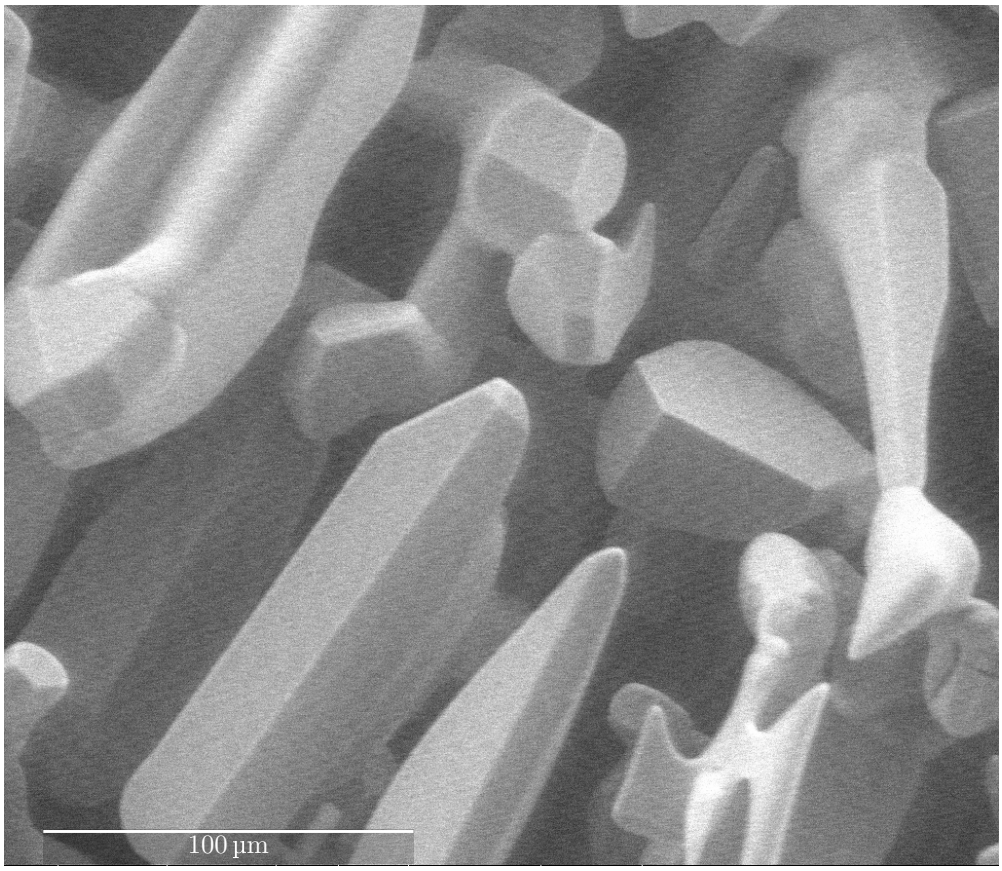

FIG. 1: Frost grown from vapour is highly faceted and formed of large single crystals that appear on top of the bulk ice grown from melt, in comparison to the polycrystalline grains seen in Figure 2 of the main text.

II. LABELLED FEATURES

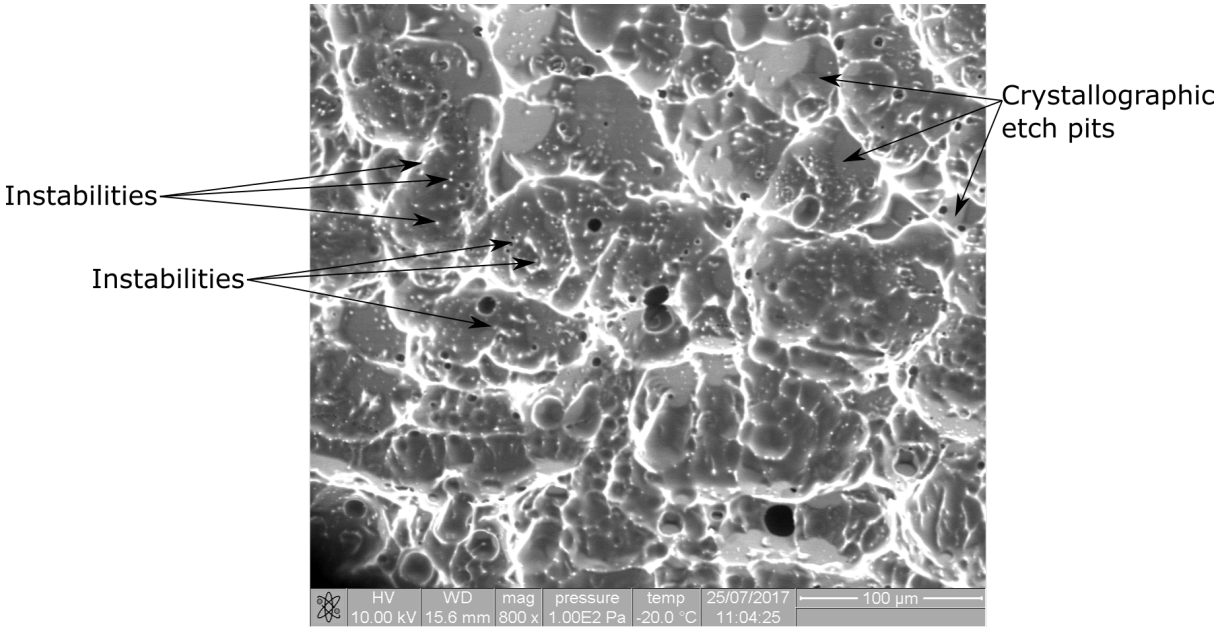

(a) Initial sublimation

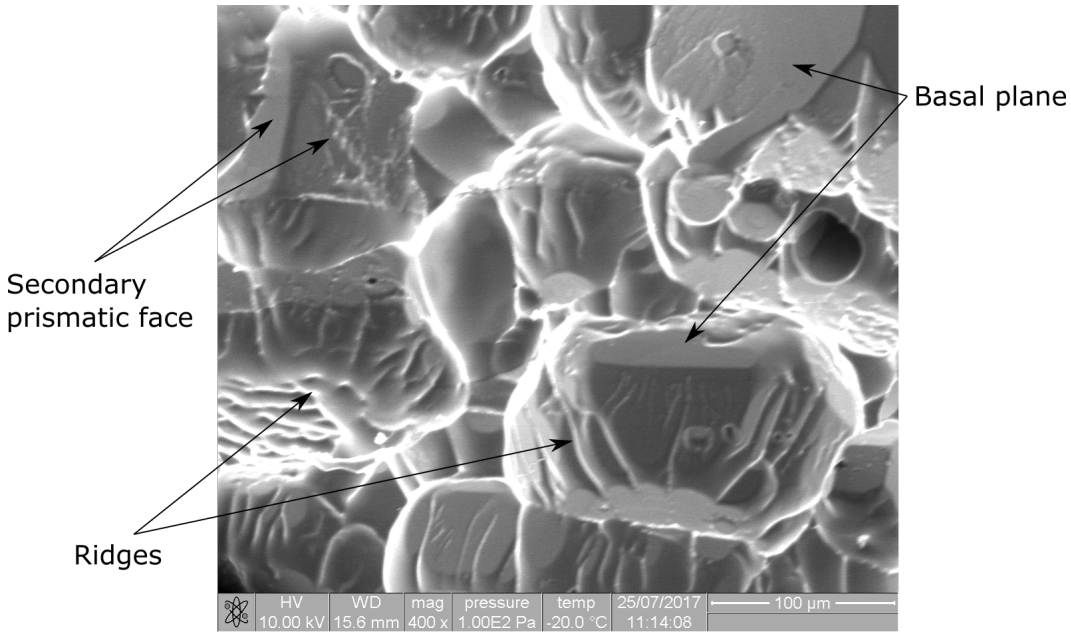

(b) Late Sublimation

FIG. 2: Labelled features including instabilities, etch pits, basal and secondary prismatic planes observed during initial and late sublimation at as seen in Figure 2

III. DISTRIBUTION OF RIDGE SPACINGS

It is interesting to note that the distribution of measured wavelengths widens with lower ΔP as seen in Figure 3. The standard deviation of this distribution, however, remains roughly unchanged when viewed through the log-log plot in the main text, Figure 5.

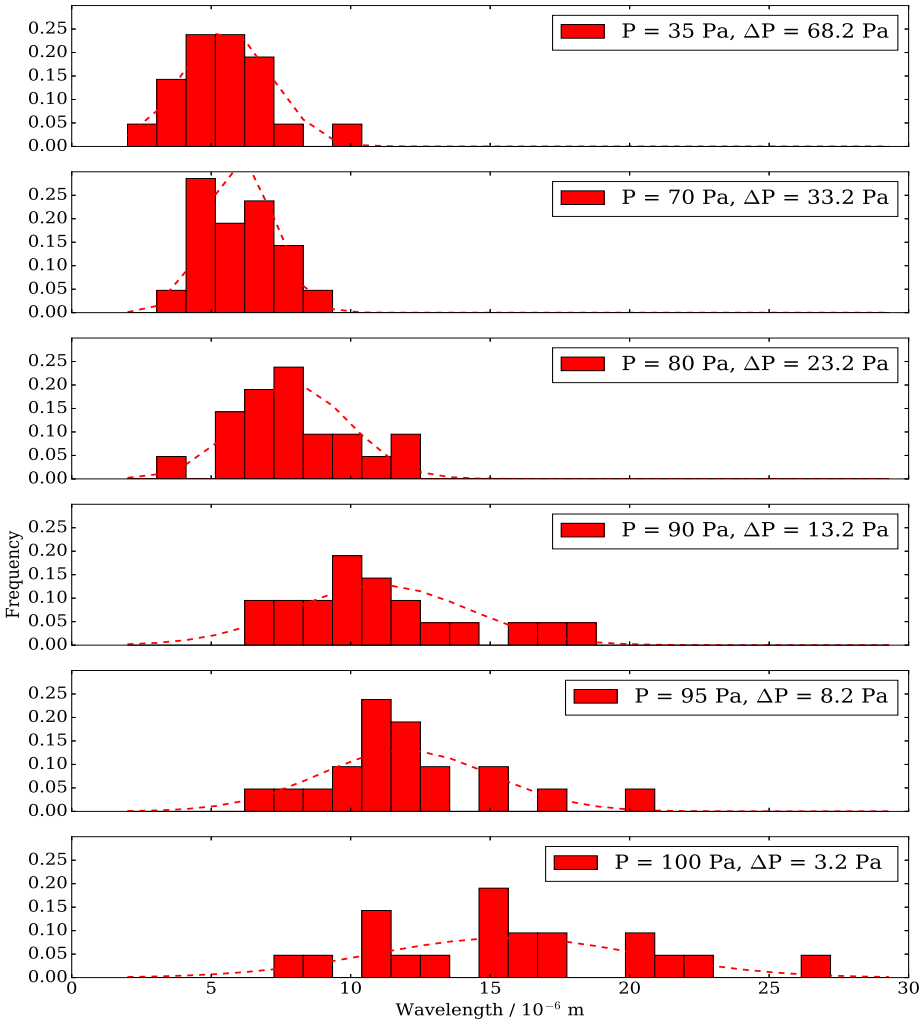

FIG. 3: The normalised distribution of the sublimation ridge wavelengths. Measurement of ridge spacings have not been corrected for polycrystalline geometry effects, resulting in the negative skew of all distributions. Holding the same direction of skew has allowed the measured spacings to ensure consistency between measurements for the purpose of illustrating the effect of pressure on ridge spacings, although absolute accuracy is not achieved.

IV. DISTRIBUTION OF SUBLIMATION VELOCITIES

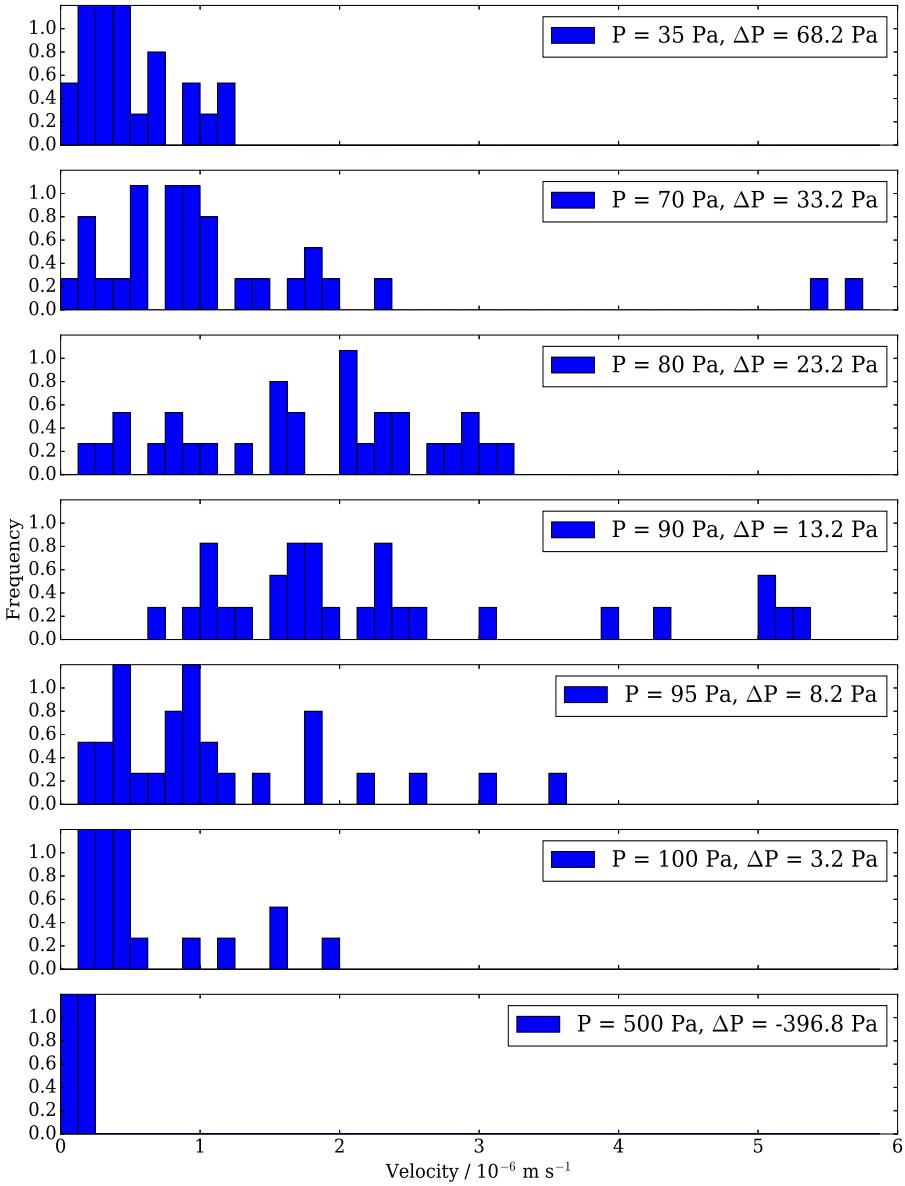

FIG. 4: The normalised distribution of the sublimation ridge velocities. Measurement of ridge velocities have not been corrected for polycrystalline geometry effects. It is worth noting that although the velocities represented here might appear to be normally distributed within the sampled fronts, the velocities represented here are captured at a line capture exposure of 3–30 μs. As a consequence, we do not have the time resolution to be able to measure the fastest moving sublimation fronts.

V. MULLINS-SEKERKA ANALYSIS

The results of the Mullins-Sekerka analysis could be used to distinguish between the spacing of dendritic features that arise from a thermally driven process like ice growth from melt and those that arise from a solute-driven process such as the sublimation of ice. The plane front for either phenomenon can be considered to be destabilised by a thermal or solute gradient but stabilised by the curvature of the front. For a perturbation to the diffusion field (either temperature or solute), there is a critical wavelength λ_s above which these perturbations are non-zero, and there exists a wavelength λ_o for which the perturbation is maximal.

In a physical representation, this wavelength λ_o is often noted to be $\sim \sqrt{3}\lambda_s$. Since this wavelength represents the fastest growing instability, it is the primary wavelength that is observed; instabilities of any other wavelengths that exist are often outgrown by those of wavelength λ_o.

In the thermally driven case, dendrite spacings can be predicted by using the result of the Mullins-Sekerka planar instability[16] where

$$\lambda_o \sim 2\pi\sqrt{3}\sqrt{(1+\beta)(\frac{D_L d_0}{V})} \tag{1}$$

$$\beta_{\text{thermal}} = \frac{D_T^S C_P^S}{D_T^L C_P^L} \tag{2}$$

$$d_{0,\text{thermal}} = \frac{\gamma T_M C_P^L}{L^2} \tag{3}$$

where V is the front velocity, γ is the surface energy, D_T^L is the thermal diffusivity of the liquid, D_T^S is the thermal diffusivity of the solid, L is the latent heat of fusion, T_M is the melting point, C_P^L is the heat capacity of the liquid at constant pressure, and C_P^S is that of the solid.

In solute driven systems, these values are replaced by:

$$\beta_{\text{chemical}} = \frac{D_C^S C_P^S}{D_C^L C_P^L} \tag{4}$$

$$d_{0,\text{chemical}} = \frac{\gamma}{(\Delta C)^2(\frac{\partial \mu}{\partial C})} \tag{5}$$

γ	3.96×10^{-2} Nm^{-1}[33]
D_L	1.31×10^{-7} $\mathrm{m}^2\mathrm{s}^{-1}$ [34]
D_S	1.045×10^{-6} $\mathrm{m}^2\mathrm{s}^{-1}$ [34]
L	3.33×10^{5} Jm^{-3} [35]
T_M	273.15 K [36]
C_P^L	5.992×10^{3} $\mathrm{Jm}^{-3}\mathrm{K}^{-1}$[37]
C_P^S	1.922×10^{3} $\mathrm{Jm}^{-3}\mathrm{K}^{-1}$[36]

TABLE I: Values of thermodynamic parameters used to calculate Mullins-Sekerka wavelengths in the thermally driven ice growth process.

where D_L is the thermal diffusivity of the liquid, D_C^L is the mass diffusivity of the liquid, D_T^S is the mass diffusivity of the solid, μ is the chemical potential, C is the concentration and ΔC is the miscibility gap.

Measurements of the growth velocity of supercooled ice have previously been estimated to be as low as 80 μm s^{-1} when controlled[31] to as high as 1 cm s^{-1}[32]. In conjunction with the thermodynamic parameters for ice and water as listed in Table I, λ_o was estimated to therefore be in range of 100–1200 μm. This value is larger than the average grain size under such conditions (∼100 μm) and therefore no dendritic growth from solidification is observed in the microstructures above.

A similar estimate of the sublimation process however, cannot accurately be made by simply considering the results of Mullins-Sekerka. Unlike most other phenomena, this particular case of sublimation and solidification is disparate;the solidification process is entirely governed by the thermal gradient whereas sublimation is a solute driven process. There is no miscibility gap in sublimation since there is neither an isobaric nor isothermal field over which both ice and water vapour coexist. Thus, the results of the Mullins and Sekerka analysis cannot be used to account for the observations noted above.

REFERENCES

[16] J. S. Langer, Reviews of Modern Physics **52**, 1 (1980).

[31] H. Zhang, I. Hussain, M. Brust, M. F. Butler, S. P. Rannard, and A. I. Cooper, Nature

Materials 4, 787 (2005).

[32] W. Macklin and B. Ryan, Philosophical Magazine **17**, 83 (1968).

[33] C. Van Oss, R. Giese, R. Wentzek, J. Norris, and E. Chuvilin, Journal of Adhesion Science and Technology **6**, 503 (1992).

[34] D. James, Journal of Materials Science **3**, 540 (1968).

[35] R. Feistel and W. Wagner, Journal of Physical and Chemical Reference Data **35**, 1021 (2006).

[36] R. Feistel, IAPWS, Doorwerth, The Netherlands, September (2009).

[37] V. Holten, J. V. Sengers, and M. A. Anisimov, Journal of Physical and Chemical Reference Data **43**, 043101 (2014).